

Conduction-band offsets in pseudomorphic $\text{In}_x\text{Ga}_{1-x}\text{As}/\text{Al}_{0.2}\text{Ga}_{0.8}\text{As}$ quantum wells ($0.07 \leq x \leq 0.18$) measured by deep-level transient spectroscopy

N. Debbar, Dipankar Biswas,* and Pallab Bhattacharya

*Solid State Electronics Laboratory, Department of Electrical Engineering and Computer Science,
The University of Michigan, Ann Arbor, Michigan 48109-2122*

(Received 27 February 1989)

The variation of the potential of a quantum well is similar to that of a deep trap. In that respect a quantum well can capture and emit carriers in much the same way as a trap. The thermal emission energy from a quantum well is closely related to the appropriate band offset. With that in mind, we have carried out deep-level transient spectroscopy measurements on Schottky-barrier diodes containing one or more pseudomorphic $\text{In}_x\text{Ga}_{1-x}\text{As}/\text{Al}_{0.2}\text{Ga}_{0.8}\text{As}$ ($0 < x \leq 0.18$) quantum wells. The objective was to estimate the conduction-band offset, ΔE_c , as a function of x and the resulting strain. From detailed balance between emission and capture, an Arrhenius-type expression was derived to analyze the transient emission data. It is seen that the percentage band offset $\Delta E_c/\Delta E_g$ varies from 62% for $x = 0.07$ to 70% at $x = 0.18$. Furthermore, a linear interpolation of the data leads to $\Delta E_c/\Delta E_g = 58\%$ at $x = 0$, which is close to the widely accepted value. Our results support recent theoretical calculations from which a monotonic increase in ΔE_c with strain in this heterostructure system is predicted.

I. INTRODUCTION

One of the most important parameters for the design of heterojunction and quantum-well electronic and optoelectronic devices is the heterojunction band offset. The band discontinuity not only depends on the semiconductors involved, but, as recently suggested,¹ also depends on the amount of mismatch strain at the interface.

Several electrical and optical techniques have been used to estimate the band offsets. In this respect the most commonly investigated heterojunctions are the lattice-matched $\text{GaAs}/\text{Al}_x\text{Ga}_{1-x}\text{As}$ and $\text{In}_{0.53}\text{Ga}_{0.47}\text{As}/\text{InP}$ heterojunctions, for their current importance. Even in these lattice-matched cases, there is considerable disagreement in the offsets estimated by different groups. Very little has been reported on the experimental determination of band offsets in pseudomorphic, lattice-mismatched heterojunctions, and, in particular, the $\text{In}_x\text{Ga}_{1-x}\text{As}/\text{GaAs}$ or $\text{In}_x\text{Ga}_{1-x}\text{As}/\text{Al}_y\text{Ga}_{1-y}\text{As}$ systems. Calculations made by Coon and Liu¹ suggest that in the $\text{In}_x\text{Ga}_{1-x}\text{As}/\text{GaAs}$ system the conduction-band offset, ΔE_c , will increase with increasing In content (i.e., strain). Reed *et al.*² have directly measured ΔE_c in $\text{In}_x\text{Ga}_{1-x}\text{As}/\text{Al}_y\text{Ga}_{1-y}\text{As}$ double-barrier resonant tunneling structures and Kowalczyk *et al.*³ have also measured the offset in the InAs/GaAs system using x-ray photoelectron spectroscopy. The percentage of conduction-band discontinuities obtained by these authors are extremely high, in the range 84–100% of ΔE_g , the band-gap difference.

The three-dimensional potential variation of a deep-level trap in the lattice of a semiconductor is similar to that of a two-dimensional quantum well, with some important and obvious differences. Quantum wells can therefore capture and emit carriers from the barrier regions in much the same way as deep levels do. In fact,

some early experiments on $\text{GaAs}/\text{Al}_x\text{Ga}_{1-x}\text{As}$ quantum wells have been made to determine the emission energy of electrons from them.⁴ Similar measurements have also been reported by Lang *et al.*,⁵ who used deep-level transient spectroscopy (DLTS) and admittance spectroscopy to estimate the valence-band offset in $\text{In}_{0.53}\text{Ga}_{0.47}\text{As}/\text{InP}$ quantum wells. It is important to realize that in doing DLTS measurements with quantum wells, it should be ensured that carrier emission from deep levels in the barrier and well regions does not mask the expected emissions from the quantum wells. A perfect example of this, which we have confirmed during our measurements, is seen in doing the measurements with $\text{GaAs}/\text{Al}_x\text{Ga}_{1-x}\text{As}$ ($x \geq 0.24$) quantum wells. Electron emission from the quantum well is masked in the DLTS data by electron emission from the dominant DX center traps⁶ in $\text{Al}_x\text{Ga}_{1-x}\text{As}$.

With the last point in mind, and with the objective of estimating the conduction-band offsets in pseudomorphic $\text{In}_x\text{Ga}_{1-x}\text{As}/\text{Al}_{0.2}\text{Ga}_{0.8}\text{As}$ ($0 < x \leq 0.2$) quantum wells, we have made systematic DLTS measurements on specially designed heterostructures grown by molecular-beam epitaxy. The thermal energy of emission has been determined as a function of In content, x , from an Arrhenius expression, to be discussed in the next section. The trend of the band offset with increasing x is approximately calculated from the measured emission energies, and it is seen that the value of $\Delta E_c/\Delta E_g$ slowly and monotonically increases with x in these pseudomorphic quantum wells.

II. THERMAL EMISSION OF ELECTRONS FROM A QUANTUM WELL

The emission rate of electrons from a quantum well can be derived from the thermionic emission current due

to electrons emitted from the well to the barrier region. This emission rate has been calculated by Martin *et al.*⁴ and is given by

$$e_n = \left[\frac{kT}{2\pi m_w^*} \right]^{1/2} \frac{1}{L_w} \exp \left[-\frac{\Delta E_c}{kT} \right]. \quad (1)$$

It is also possible, by drawing an analogy between an electron quantum well and a deep-level trap, to formulate a detailed balance between thermal capture and emission of electrons from the quantum wells.⁷ The capture rate of electrons into the well, r_{cn} , is proportional to the electron concentration in the barrier, n_B , and to the empty states in the well, \bar{n}_w :

$$r_{cn} = \langle v_{th} \rangle \chi n_B \bar{n}_w, \quad (2)$$

where $\langle v_{th} \rangle$ is the average thermal velocity of electrons, and χ (cm²) is a capture cross section related to the scattering rate of carriers into the well. It is, therefore, closely related to the quantum-well parameters. By using a three-dimensional density of states in the well, which is approximately valid for $L_w \geq 150$ Å,

$$\bar{n}_w = (8\pi/3h^3)(2m_w^*)^{3/2}(\Delta E)^{3/2}, \quad (3)$$

where ΔE is the difference in energy between the first electron subband and the top of the well. Similarly,

$$n_B = N_{CB} \exp[(E_f - E_{CB})/kT], \quad (4)$$

where N_{CB} is the three-dimensional density of states in the barrier material. The emission rate of electrons from the well, r_{en} , is given by the product of the emission probability e_n and the number of electrons, n_w , in the well. In other words,

$$r_{en} = e_n \frac{4\pi}{h^3} (2m_w^*)^{3/2} \frac{\sqrt{\pi}}{2} (kT)^{3/2} \exp \left[\frac{E_f - E_{CW}}{kT} \right]. \quad (5)$$

In thermal equilibrium,

$$r_{en} = r_{cn}. \quad (6)$$

By substituting Eqs. (1)–(4) in (5),

$$e_n = \frac{16\pi^{3/2}}{3h^3} m_B^* \chi (kT)^{1/2} (\Delta E)^{3/2} \exp \left[-\frac{\Delta E}{kT} \right]. \quad (7)$$

It is clear that, although the exponential dependence is identical in Eqs. (1) and (7), there are important differences in the prefactor. This difference comes mainly from the fact that in the thermionic emission model the electrons in the wells must have an energy greater than ΔE_c to be thermally emitted over the barrier.

Next, consider a single quantum well (SQW) in the depletion region of a Schottky barrier, as shown in Fig. 1. The existence of confined electrons in the well changes the depletion width W . Solution of Poisson's equation in the well and barrier regions with the appropriate boundary conditions gives⁸

$$W^2 = W_0^2 (1 + 2n_w LL_w / N_D W_0^2), \quad (8)$$

where $W_0^2 = (2\epsilon/qN_D)V$ is the depletion region width in

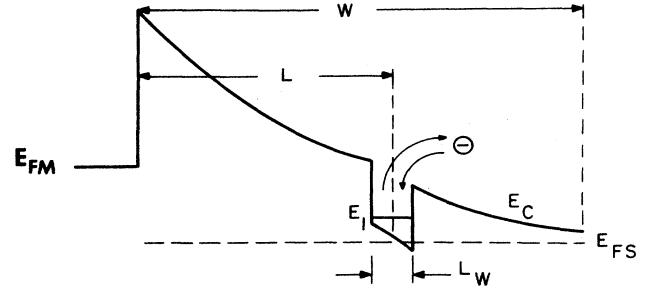


FIG. 1. Band diagram of a reverse-biased Schottky diode with a SQW in the depletion region.

the absence of the well. N_D is the net donor density in the barrier, and $V = V_{app} + V_{bi}$, where V_{bi} is the built-in voltage and V_{app} is the applied bias. The transient capacitance ΔC is then given by

$$\Delta C / C(W) \approx n_w LL_w / N_D W_0^2. \quad (9)$$

The DLTS signal for rate windows t_1 and t_2 (Ref. 9) is then given by

$$s(t) = C(t_2) - C(t_1) \\ = C_0 \frac{n_{w0}}{N_D} \frac{LL_w}{W_0^2} [\exp(-e_n t_1) - \exp(-e_n t_2)]. \quad (10)$$

III. EXPERIMENTAL TECHNIQUES

Five samples of pseudomorphic $\text{In}_x\text{Ga}_{1-x}\text{As}/\text{Al}_y\text{Ga}_{1-y}\text{As}$ SQW's and double quantum wells (DQW's) were grown by molecular-beam epitaxy (MBE) on Si-doped (100)-oriented GaAs substrates in a Varian Gen II system. The structures were uniformly doped in the range $(1-5) \times 10^{16}$ cm⁻³. The schematics in the SQW and DQW structures, listed in Table I, are shown in Figs. 2(a) and 2(b), respectively. The first sample has a 150-Å $\text{In}_{0.2}\text{Ga}_{0.8}\text{As}$ well and an $\text{Al}_{0.16}\text{Ga}_{0.84}\text{As}$ barrier. In the other four samples the well thickness of 120 Å and the $\text{Al}_{0.2}\text{Ga}_{0.8}\text{As}$ barrier composition was kept constant while the In composition in the well region was varied. Gold Schottky barriers with an area of 2.2×10^{-3} cm² were formed on the heterostructure by evaporation. These structures have the following advantages. $\text{Al}_x\text{Ga}_{1-x}\text{As}$ with $x \leq 0.24$ does not have the DX center. The traps in strained $\text{In}_{0.2}\text{Ga}_{0.8}\text{As}$ have been identified by us and none

TABLE I. Description of the quantum-well structures for DLTS measurements.

Sample No.	Well thickness (Å)	Well compos.	Barrier compos.
1	150	$\text{In}_{0.2}\text{Ga}_{0.8}\text{As}$	$\text{Al}_{0.16}\text{Ga}_{0.84}\text{As}$
2	120	$\text{In}_{0.13}\text{Ga}_{0.87}\text{As}$	$\text{Al}_{0.2}\text{Ga}_{0.8}\text{As}$
	120	$\text{In}_{0.18}\text{Ga}_{0.82}\text{As}$	$\text{Al}_{0.2}\text{Ga}_{0.8}\text{As}$
3	120	$\text{In}_{0.1}\text{Ga}_{0.9}\text{As}$	$\text{Al}_{0.2}\text{Ga}_{0.8}\text{As}$
4	120	$\text{In}_{0.15}\text{Ga}_{0.85}\text{As}$	$\text{Al}_{0.2}\text{Ga}_{0.8}\text{As}$
5	120	$\text{In}_{0.07}\text{Ga}_{0.93}\text{As}$	$\text{Al}_{0.2}\text{Ga}_{0.8}\text{As}$

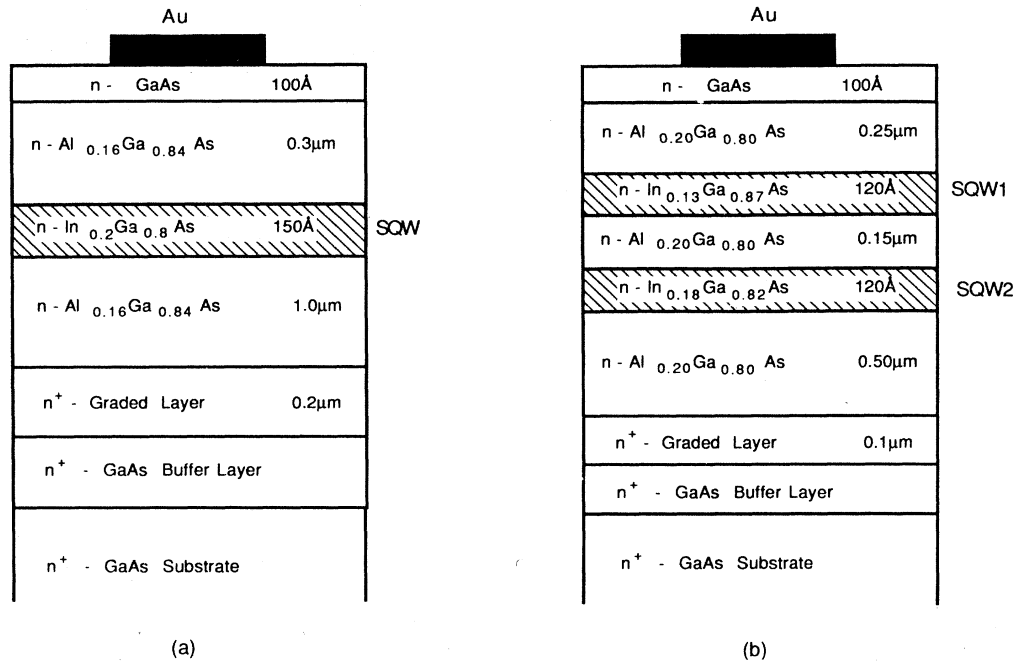


FIG. 2. Schematics of (a) single-quantum-well and (b) double-quantum-well Schottky diodes grown by molecular-beam epitaxy.

of the identified centers occur in the range where the emissions from the quantum well are expected. The doping and thickness of the heterostructure layers were carefully controlled, so that the quantum wells are outside the zero-bias depletion region, but could be brought into the depletion region with the quiescent reverse bias used in the experiments. The diodes have a typical reverse

breakdown voltage of 12–15 V. Capacitance-voltage measurements give a value of $N_D \approx 1.5 \times 10^{16} \text{ cm}^{-3}$ for the first sample and $N_D \approx 4 \times 10^{16} \text{ cm}^{-3}$ for the other four samples. The depletion-accumulation regions observed due to the SQW, in a particular sample, as seen in the capacitance-voltage data, are shown in Fig. 3. DLTS measurements were carried out with a variable-temperature cryostat, a 1-MHz Boonton capacitance meter, and a signal analyzer for providing the rate windows and processing the capacitance-difference signals with varying temperatures.

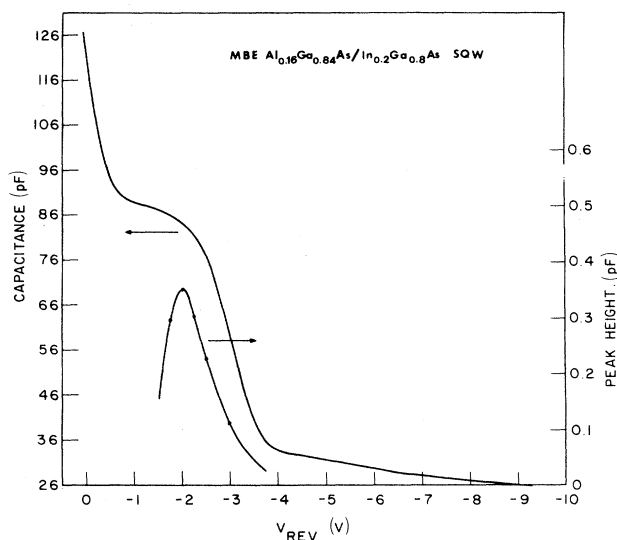


FIG. 3. Variation of depletion-layer capacitance and DLTS peak height of the quantum-well emission with bias applied to the diode.

IV. RESULTS

The prominent peak obtained in the DLTS temperature scan of the first sample, originating from the quantum well, is shown in Fig. 4. An important observation is the fact that the height of the DLTS peak passes through a maximum at almost the same reverse bias at which the depletion accumulation is observed in the capacitance-voltage curve of Fig. 3. By repeating the DLTS scan with varying rate windows, an Arrhenius plot is obtained. The emission activation energy ΔE , in accordance with Eq. (7), is proportional to the slope of the Arrhenius plot and is found to be 0.204 eV for this sample. By adjusting the quiescent reverse bias to the Schottky diode, the DLTS data corresponding to the $\text{Al}_{0.16}\text{Ga}_{0.84}\text{As}$ barrier region could be observed. The traps corresponding to the emissions from the barrier materials have been previously observed by us and other authors^{10–12} in bulk $\text{Al}_y\text{Ga}_{1-y}\text{As}$ of the same composition. Furthermore, upon repeating the measurement with a diode made on a sample with the quantum well etched off, the same DLTS

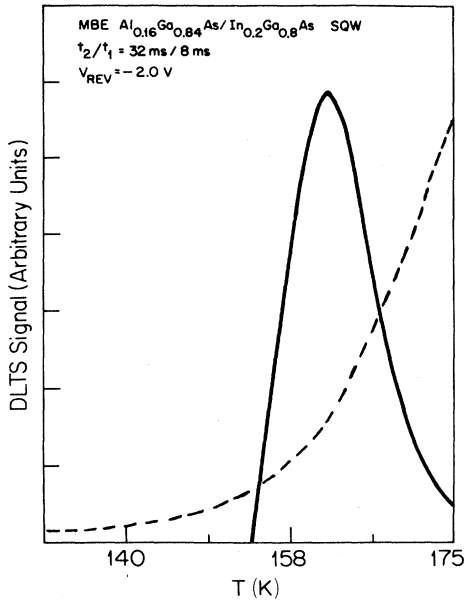


FIG. 4. DLTS signal resulting from thermal emission of electrons from the quantum well. The dashed profile indicates DLTS data obtained from the same sample with the quantum well removed.

data were obtained, as shown in Fig. 5. It is important to note that the peak that we believe results from quantum-well emissions (Fig. 4) is noticeably absent in the data of Fig. 5. It is important to mention one of our observations here. It was generally found that the overall DLTS signal amplitude over the entire range of scanned temperature is

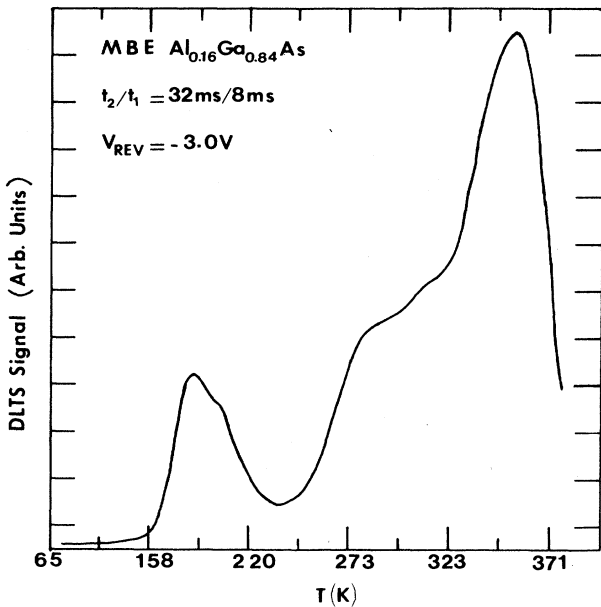


FIG. 5. DLTS data of molecular-beam-epitaxy-grown $\text{Al}_{0.16}\text{Ga}_{0.84}\text{As}$ obtained with a Schottky diode reverse biased at ~ 3 V.

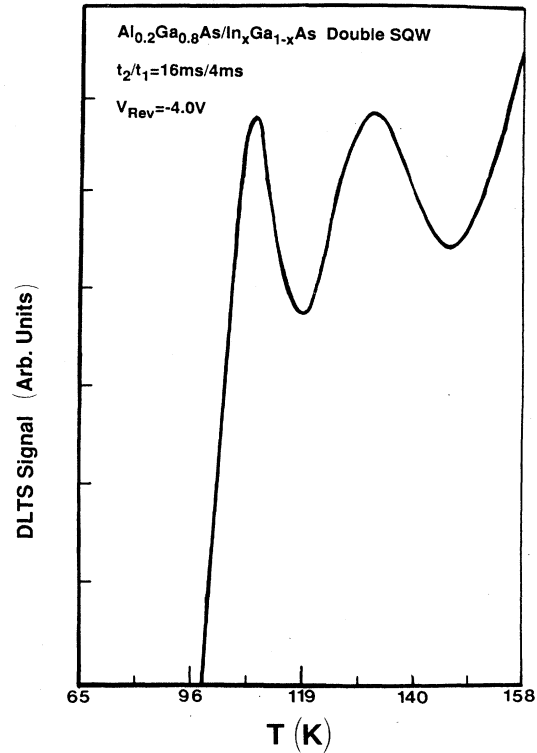


FIG. 6. DLTS signal resulting from thermal emission of electrons from the quantum wells of different compositions (sample 2).

higher in the samples with the quantum wells than that in samples without the quantum wells. We believe the higher background signal in the former case results from the emission from distributed interface states of the quantum well.

Upon performing the DLTS measurements with a sample having two quantum wells of different compositions, two prominent peaks, as shown in Fig. 6, were observed. It is to be noted that there is no negative-going peak below 100 K in the data. On repeating the experiments with varying rate windows, data for the Arrhenius plots

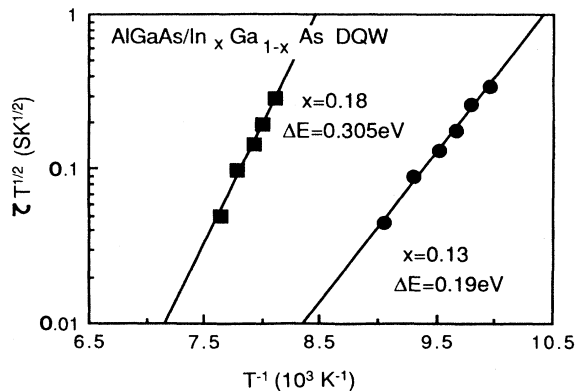


FIG. 7. Arrhenius plots corresponding to emissions from $\text{In}_{0.13}\text{Ga}_{0.87}\text{As}$ and $\text{In}_{0.18}\text{Ga}_{0.82}\text{As}$ quantum wells.

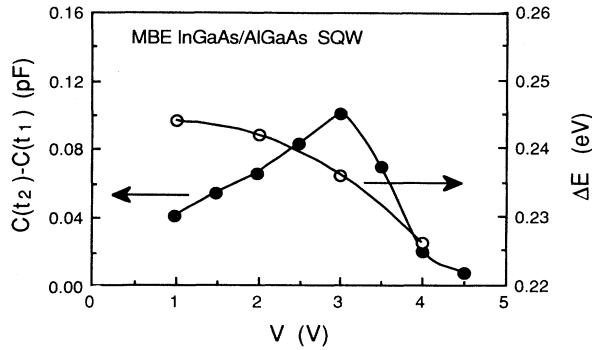


FIG. 8. Variation of DLTS peak height and activation energy of the quantum-well emission with bias applied to the diode.

are obtained, and these plots are shown in Fig. 7. From the slopes, values of $\Delta E = 0.19$ and 0.305 eV are obtained. The fact that the number of peaks increase with the number of quantum wells incorporated in the device lends enough credence to the fact that the low-temperature peaks shown in Figs. 4 and 6 result from electron emission from the quantum wells.

Finally, Fig. 8 shows the effect of varying reverse bias on quantum-well-emission properties for a SQW sample. The DLTS signal peak goes through a maximum and, at the same bias, the rate of change of the emission energy, ΔE , is a maximum. The reduction in ΔE is due to change in the band bending and field-enhanced tunneling from the well. The change in ΔE will change the emission rates through Eq. (7).

V. DISCUSSION

As stated earlier, our main objective is to estimate the trend in the band offsets of $\text{In}_x\text{Ga}_{1-x}\text{As}/\text{Al}_y\text{Ga}_{1-y}\text{As}$ quantum wells with increasing x . The thermal emission energy ΔE is related to the conduction-band offset ΔE_c of the $\text{In}_x\text{Ga}_{1-x}\text{As}/\text{Al}_y\text{Ga}_{1-y}\text{As}$ heterostructure. We have therefore estimated the values of ΔE_c for varying x , by adding to ΔE the band bending due to the electric field F and the first subband energy E_{e1} . In other words,

$$\Delta E_c \simeq \Delta E + E_{e1} + L_w F. \quad (11)$$

There are obvious sources of error in this simple formulation, the principal ones being the spread in the subband energies and the excess energy of carriers above the barrier during emission, or reduced energy due to tunneling. The value of E_{e1} was obtained from theoretical analysis. Next, ΔE_g was obtained from theoretical calculations which include the effects of strain in the pseudomorphic well and the bowing in the band-gap energies of the InAs-GaAs system. Experimentally, ΔE_g was estimated from photoluminescence measurements by determining the energy position of the transitions from the $\text{Al}_y\text{Ga}_{1-y}\text{As}$ band edge and from the $E_{e1} - E_{hh1}$ transition of the $\text{In}_x\text{Ga}_{1-x}\text{As}$ quantum well. The measured values of ΔE_g agree well with the theoretical estimates.

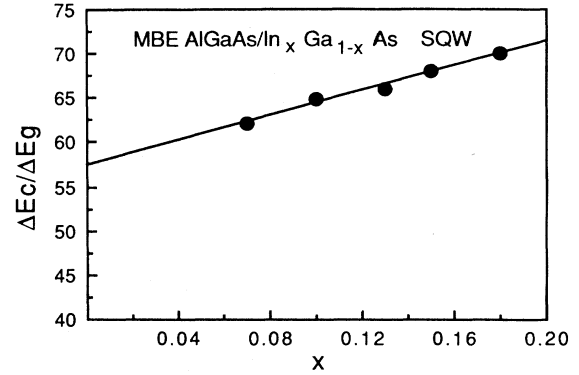


FIG. 9. Measured variation of conduction-band offset with composition x for $\text{In}_x\text{Ga}_{1-x}\text{As}/\text{Al}_{0.2}\text{Ga}_{0.8}\text{As}$ quantum wells.

Figure 9 shows the plot of $\Delta E_c/\Delta E_g$ versus In composition x . It is clear that the offset increases monotonically with increase in x , reaching a value of 0.7 at $x = 0.18$. It is also important to note that the values extrapolate to $\Delta E_c/\Delta E_g \simeq 0.6$ for $x = 0$. Therefore it is apparent that biaxially compressive strain tends to increase the value of ΔE_c , as suggested by recent theoretical work.¹ Experimentally, the offsets in this pseudomorphic system have been measured by Reed *et al.*² and by Kowalczyk *et al.*³ for InAs-GaAs. The values of $\Delta E_c/\Delta E_g$ reported by these groups of authors are higher (84–100%). Taking into account the likely sources of error in our measurements, the error bar in ΔE may be ± 10 – 15 meV.

We have recently made intersubband absorption measurements¹³ on $\text{In}_x\text{Ga}_{1-x}\text{As}/\text{Al}_{0.4}\text{Ga}_{0.6}\text{As}$ ($0 \leq x \leq 0.15$) MQW waveguide samples using Fourier-transform infrared spectroscopy. The intersubband transition energy was determined for 50-Å wells and, from the analyses of the data, the values of ΔE_c were estimated. These values are very close to those determined from the DLTS measured and shown in Fig. 9, taking into account the important differences in the quantum-well parameters in the two sets of measurements.

It may therefore be said, in conclusion, that the class of transient measurement techniques, which include capacitance and admittance spectroscopy, are very suitable for the determination of the band offsets in suitably designed samples with a fair amount of accuracy. We have used the DLTS technique to estimate the trend in the offset of pseudomorphic $\text{In}_x\text{Ga}_{1-x}\text{As}/\text{Al}_y\text{Ga}_{1-y}\text{As}$ quantum wells. Our results indicate that over the range of In composition that we have examined, the values of $\Delta E_c/\Delta E_g$ slowly increases from ~ 0.6 , the value for lattice-matched GaAs/ $\text{Al}_y\text{Ga}_{1-y}\text{As}$, to ~ 0.7 for $x = 0.18$.

ACKNOWLEDGMENTS

We would like to thank Dr. J. E. Oh for providing the samples. This work was supported by the U.S. National Science Foundation (Materials Research Group Program) under Grant No. DMR-86-02675.

- *On leave from Institute of Radiophysics and Electronics, 92 Acharya Prafulla Road, Calcutta 700009, West Bengal, India.
- ¹D. D. Coon and H. C. Liu, *J. Appl. Phys.* **60**, 2893 (1986).
- ²M. A. Reed and J. W. Lee, *Appl. Phys. Lett.* **50**, 845 (1987).
- ³S. P. Kowalczyk, W. J. Schaffer, E. A. Kraut, and R. W. Grant, *J. Vac. Sci. Technol.* **20**, 705 (1982).
- ⁴P. A. Martin, K. Meehan, P. Gavrilovic, K. Hess, N. Holonyak, and J. J. Coleman, *J. Appl. Phys.* **54**, 4689 (1983).
- ⁵D. V. Lang, in *Heterojunction Band Discontinuities: Physics and Device Applications*, edited by F. Capasso and G. Margaritondo (Elsevier, Amsterdam, 1987).
- ⁶S. Dhar, W. P. Hong, P. Bhattacharya, Y. Nashimoto, and F. Y. Juang, *IEEE Trans. Electron Devices* **ED-33**, 698 (1986).
- ⁷N. Debbar and P. Bhattacharya, *J. Appl. Phys.* **62**, 3845 (1987).
- ⁸B. Hamilton, K. E. Singer, and A. R. Peaker, in *Proceedings of the Twelfth International Symposium on Gallium and Related Compounds, Karinzawa, Japan*, edited by M. Fujimoto (The Institute of Physics, London, 1986), p. 241.
- ⁹D. V. Lang, *J. Appl. Phys.* **45**, 3023 (1974).
- ¹⁰S. Dhar, U. Das, and P. Bhattacharya, *J. Appl. Phys.* **60**, 639 (1986).
- ¹¹K. Hikosaka, T. Mimura, and S. Hiyamizu, in *Proceedings of the Eighth International Symposium on Gallium Arsenide and Related Compounds, Vienna*, edited by H. Thirn (The Institute of Physics, London, 1981), p. 233.
- ¹²K. Yamanaka, S. Naritsuka, K. Kanamoto, M. Mihara, and M. Ishii, *J. Appl. Phys.* **61**, 5062 (1987).
- ¹³X. Zhou, P. K. Bhattacharya, G. Hugo, S. C. Hong, and E. Gulari, *Appl. Phys. Lett.* **54**, 855 (1989).